Eurasian Journal of Physics and Functional Materials

2020, 4(3), 261-267

Photoelectric properties of TiO_2-GO+Ag ternary nanocomposite material

N.Kh. Ibrayev[1], A.Zh. Zhumabekov*[,1,2], E.V. Seliverstova[1]

[1]Institute of Molecular Nanophotonics, Buketov Karaganda University, Karaganda, Kazakhstan

[2]Toraighyrov University, Pavlodar, Kazakhstan

E-mail: almar89-89@mail.ru

DOI: **10.29317/ejpfm.2020040309**
Received: 04.08.2020 - after revision

A ternary nanocomposite material based on TiO_2, graphene oxide and core-shell nanostructures of Ag/TiO_2 composition was obtained by a two-step hydrothermal method. The formation of a dual TiO_2-GO nanocomposite was confirmed by Raman spectroscopy data, where the nanocomposite spectra contain peaks characteristic of both TiO_2 and graphene oxide. Studies of electrophysical characteristics have shown that the addition of plasmon nanoparticles leads to an improvement in the charge-transfer characteristics of the synthesized material. This is due to the fact that the charge transfer resistance of a ternary nanocomposite material TiO_2-GO-Ag is noticeably lower than for pure TiO_2 ($\approx$ 13 times) and TiO_2-GO nanocomposite ($\approx$ 3 times). In addition, the prescence of Ag/TiO_2 core-shell nanostructures in the TiO_2-GO nanocomposite material leads to an increase in the efficiency of conversion of incident light into photocurrent, which will be resulted in the growth of photocatalytic activity of synthesized materials.

Keywords: titanium dioxide, graphene oxide, TiO_2-GO, ternary nanocomposite material, impedance spectra.

Introduction

Titanium dioxide (TiO_2) is one of the widely used semiconductor materials due to its physical and chemical properties, such as high melting point, chemical inertia, high phototransformation efficiency and photostability. It is used in photocatalysis, solar batteries and sensor technology [1-3]. One of the possible disadvantages of titanium dioxide is its optical characteristics due to the width of

its band gap, which is equal to 3.0-3.2 eV depending on the structure of anatase or rutile, which causes its light absorption and sensitivity of materials based on it mainly to ultraviolet radiation. However, this disadvantage can be significantly compensated by using a nanocomposite material based on TiO_2 and carbon materials, which can include graphene.

Graphene, due to its unique structure and electronic properties, is widely used in energy and environmental materials, such as solar energy conservation, photovoltaics, photoelectrochemical and photocatalytic generation of hydrogen/hydrocarbon fuels, and photocatalysis of organic pollutants [4-9]. In recent years, composites based on TiO_2 and graphene with its modifications have attracted a lot of attention, since they are more efficient at separating charges and transporting electrons compared to pure TiO_2 [10-13]. Graphene also absorbs both UV radiation and 1-2% of light in the visible range of the spectrum [14-18].

Interest in metal nanoparticles, in particular Ag, is related to their unique optical and electronic properties. These properties are the result of the presence of plasmon resonance in metal nanoparticles. To date, a lot of work has been done on the use of Ag nanoparticles in medicine, photocatalysis, optoelectronics, and many others [19-21].

However, the direct use of silver nanoparticles in titanium oxide and graphene films is limited by a number of factors, such as oxidation of silver nanoparticles by electrolyte and increased recombination processes in the material. This problem can be resolved by using "core-shell" nanostructures, where the core - is a silver nanoparticle, with a shell - TiO_2, which will protect the metal nanoparticle from oxidation by the electrolyte. Also, the presence of a semiconductor shell will avoid recombination processes between the metal and the electrolyte.

In this work, a ternary nanocomposite material based on TiO_2, graphene oxide and the Ag/TiO_2 "core-shell" nanostructure (NS) was synthesized. It is assumed that adding nanostructures to a double nanocomposite will improve the photovoltaic properties of the material, which can be used in photocatalysis.

Experiment

Preparation of the TiO_2-GO nanocomposite material by hydrothermal synthesis was carried out according to the method [22]. Previously, it was shown that the highest increase in charge-transport parameters and photocatalytic activity of the synthesized material were registered when the concentration of GO in relation to TiO_2 was equal to 5 wt%.

Ag/TiO_2 core-shell NS with a core diameter of 20 nm and a shell thickness of 6 nm were synthesized using the method described in [23]. The core- shell particles were added to the TiO_2 and TiO_2-GO paste and further mixed for 24 hours. After that, pastes with plasmon NS were deposited onto solid substrates using the "spin-coating" method.

Graphene oxide (SLGO, Cheaptubes), TiO_2 (d>21 nm, anatase, 99.7%, Sigma Aldrich), deionized water (purified using the Aquamax water treatment system), and ethanol (anhydrous) were used to prepare the TiO_2-GO nanocomposite

material. The films were deposited onto the surface of glass substrates coated with a conductive layer of FTO (Fluorine doped tin oxide coated glass slide, $\approx 7\,\Omega$/sq, Sigma Aldrich). Iodolyte (HI-30, Solaronix) and Meltonix (25 μm, Solaronix) were used during the assemblying of cells for electrophysical measurements. All reagents were analytically pure and used without additional cleaning.

The surface morphology of the obtained composite materials was investigated by scanning electron microscope (SEM) Tescan Mira-3 (Tescan) and transmission electron microscope (TEM) JEM-1400Plus (Jeol) with an accelerating voltage of 120 kV. The Confotec MR520 microscope (Sol Instruments) with a laser excitation at 632.8 nm was used to register Raman spectra.

The impedance spectroscopy was used to study the kinetics of transport and recombination of charge carriers. Measurement of impedance spectra was carried out under illumination of samples by xenon lamp light with radiation power of 100 mV/cm^2 (Cell Tester Model#CTAAA, Photo Emission Tech. Inc., USA) on Z-500PRO impedancemeter (Elins, Russia). The amplitude of the applied signal was equal to 25 mV, and the frequency was ranged from 1 MHz to 100 mHz.

The photocatalytic activity of the obtained materials was studied by registering the photoinduced current in a standard photoelectrochemical three-electrode cell with a quartz window on a P-30J galvanostat (Elins). Ag/AgCl was used as the reference electrode. The samples was illuminated with diode lamp with a power of 35 mW/cm^2. The samples were deposited by centrifugation onto the surface of the FTO substrates that were connected to the working electrode. A platinum electrode was connected to the negative potential. The measurements were carried out in 0.1 M NaOH electrolyte.

Results and discussion

Shows the SEM image of the TiO_2-GO nanocomposite material are shown in the Figure 1. It is seen that TiO_2 nanoparticles are aggregated in a bulk sample of semiconductor. However, a small number of micropores in the images are distinguished. It is known that graphene oxide has a layered structure, which is formed by separate sheets. In hydrothermal synthesis of nanocomposite material, titanium dioxide particles tend to be less aggregated.

TEM images of the TiO_2-GO nanocomposite material also show presence of TiO_2 nanoparticles and graphene oxide sheets (Figure 1(b)). The "core-shell" nanostructures are also clearly visible on TEM images.

SEM and TEM images show that graphene oxide sheets are dispersed over the entire volume of synthesized nanocomposites. This can facilitate more efficient injection of photogenerated electrons into graphene sheets, which will ensure their further transport to the FTO layer and their registration.

To quickly identify the synthesized nanocomposite, Raman spectroscopy is used, which confirms the obtaining of the TiO_2-GO nanocomposite material. The Raman spectra of TiO_2 indicate an anatase structure that has six combinationally active peaks in the vibrational spectrum [24]. The Raman spectrum also shows D- and G- bands of graphene oxide [25]. Thus, both TiO_2 and graphene oxide

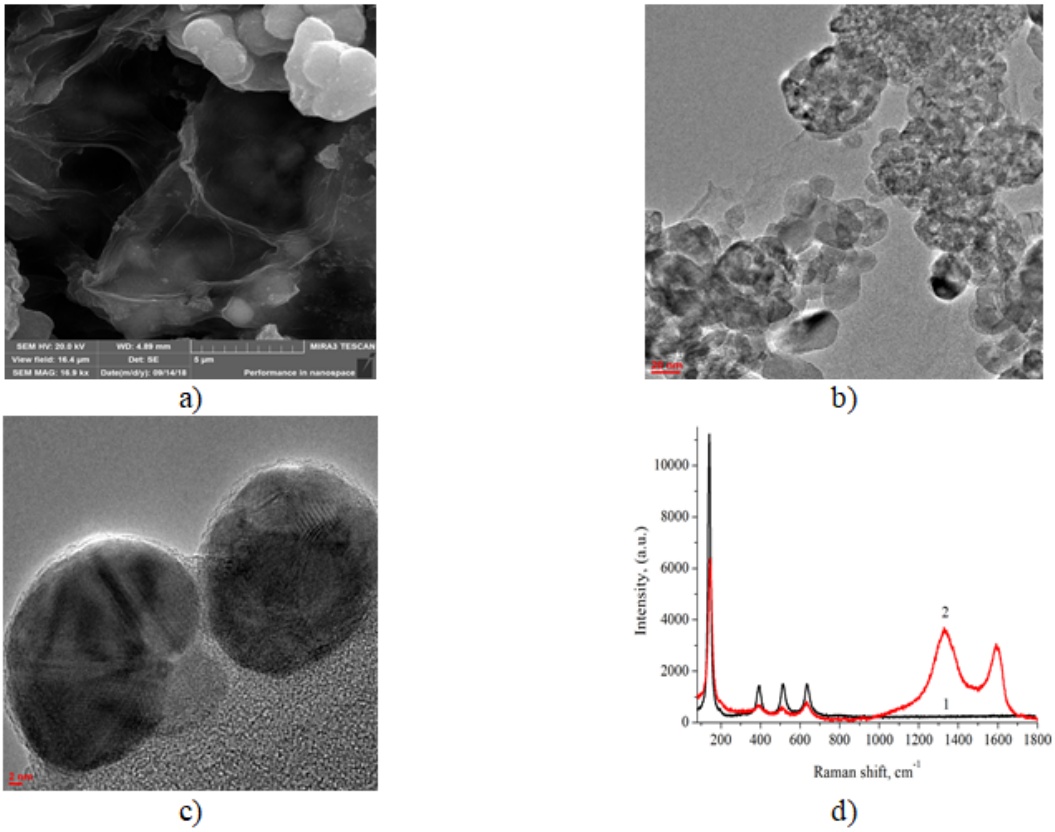

Figure 1. SEM (a) and TEM (b, c) images of the synthesized TiO_2 -GO nanocomposite (b) and the Ag/TiO_2 NS (c) and the Raman spectrum (d) of: 1-TiO_2 , 2-TiO_2 -GO.

peaks are present in the Raman spectra of the synthesized material.

Further, the electrophysical characteristics of the TiO_2-GO nanocomposite material and pure TiO_2 were studied. To obtain an equivalent circuit, data from the measured impedance spectra were processed in the EIS analyzer program. To analyze the experimental curves and evaluate the charge transport properties of films, a simple equivalent electrical circuit of an electrochemical cell was used, which is a special case of the circuit from the References [12, 26]. Figure 2(a) shows the impedance spectra of the samples. The figure shows that the lowest resistance has TiO_2-GO nanocomposite material with the addition of Ag/TiO_2 NS.

Based on the obtained data (Figure 2(a)), the charge transport properties of films were calculated, where: R_k is the charge-transport resistance related to recombination of electron, R_w is the electron transport resistance in TiO_2-GO, k_{eff} is the effective rate constant for recombination, and τ_{eff} is the effective lifetime of electrons. Table 1 shows the electrophysical parameters of the TiO_2-GO nanocomposite material.

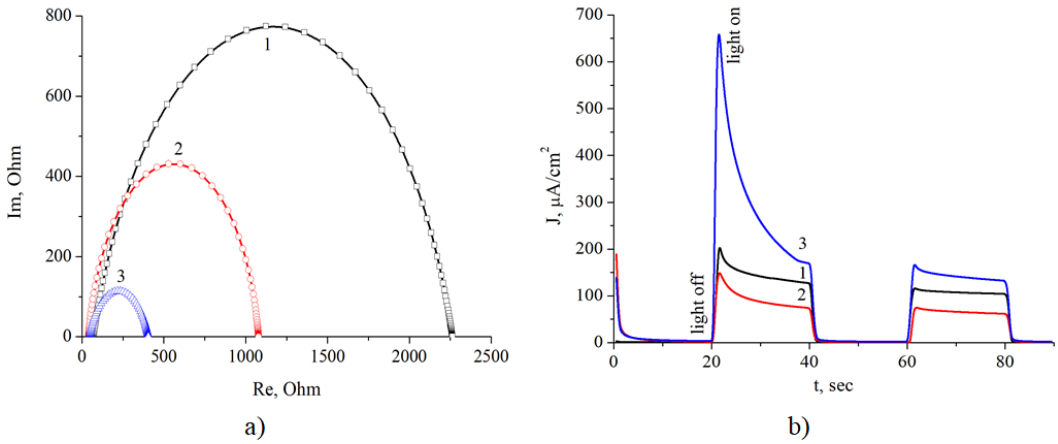

Figure 2. Impedance spectra (a) and transient characteristics of the photoinduced current of films based on: 1-TiO_2 +Ag, 2-TiO2-GO, 3-TiO_2 -GO+Ag.

Table 1.
Charge transport parameters of TiO_2, TiO_2-GO films and with the addition of Ag/TiO_2 NS.

Samples	k_{eff}, (s^{-1})	τ_{eff}, (s)	R_k, (Ohm)	R_W, (Ohm)	<J>, (mkA/cm^2)
TiO_2	0.5	2.00	29656.0	35.4	30.8
TiO_2+Ag	7.9	0.12	2229.0	33.0	61.7
TiO_2-GO	16.0	0.06	1031.0	39.0	71.4
TiO_2-GO+Ag	19.3	0.05	361.0	43.0	194.0

Table 1 show that when the core-shell NS was added to the titanium dioxide film, the charge transfer resistance decreases. The pure TiO_2 sample has the highest R_k compared to other samples. This parameter was reduced by almost 13 times under the addition of Ag/TiO_2 NS to pure TiO_2. For films based on TiO_2-GO nanocomposites, R_k has lower value. At the same time, the addition of Ag/TiO_2 NS to the TiO_2-GO nanocomposite results in a 2.8-fold decrease in R_k compared to TiO_2-GO. Thus, the impedance spectra of the obtained samples show that in the presence of Ag/TiO_2 NS in the TiO_2 and the TiO_2-GO nanocomposite results in the decreasing of the charge transfer resistance by 13 and 2.8 times, respectively.

Figure 2(b) shows the photoelectric characteristics of ternary nanocomposite materials and TiO_2, which allow us to evaluate their photocatalytic activity. The intensity of the photocurrent was measured for 20 seconds when the light was cycled on and off. It is seen, that the ternary TiO_2-GO nanocomposite with the addition of the core-shell NS shows a high photocurrent density J, which is equal to 194 μA. It is worth noting that when the sample is illuminated, the generation of photoinduced electron-hole pairs manifests itself as a large burst of photocurrent. After that, the charge carriers migrate from the inner part of the film to the surface and the activity decay. The subsequent decrease in photocurrent indicates that recombination is taking place inside the film.

Thus, performed study has shown that hydrothermal synthesis produces a nanocomposite material based on TiO_2 and graphene oxide. In the Raman

spectra of the nanocomposite exhibits maxima that are characteristic of both TiO_2 and graphene oxide.

Studies of electrophysical properties show that the addition of the Ag/TiO_2 core-shell NS to TiO_2 and the TiO_2-GO nanocomposite improves the electrophysical properties, in particular, the charge transfer resistance. It is shown that when Ag/TiO_2 was added, R_k was reduced by 13 and 2.8 times compared to neat TiO_2 and TiO_2-GO, respectively.

Studies of photovoltaic properties have shown that he generation of photoinduced current increases to an average of 194 μA in the samples based on nanocomposite with the addition of Ag/TiO_2 NS.

Thus, these parameters directly show that using of core-shell nanostructures in the TiO_2-GO nanocomposite allow to enhance the charge-transport parameters of semiconductor films, which, in turn, affect the photocatalytic activity of the synthesized material.

Acknowledgment

This work had been performed within the framework of the research grant AP05132443, funded by the Ministry of Education and Science of the Republic of Kazakhstan.

References

[1] K. Sasan et al., Nanoscale **7** (2015) 13369-13372.
[2] O. Oluwafunmilola, M. Maroto-Valer, Journal of Photochemistry and Photobiology C: Photochemistry Reviews **24** (2015) 16-42.
[3] A. Mills, S. Hunte, Journal of Photochemistry and Photobiology A: Chemistry **108** (1997) 1-35.
[4] P.V. Kamat, Journal Physics Chemistry Letters **242** (2011) 242-251.
[5] M. Ikram et al., Current Applied Physics **15** (2015) 48-54.
[6] X. Wang et al., Nano Letters **8** (2008) 323-327.
[7] M. Ikram et al., Mater. Res. Bull. **75** (2015).
[8] Z. Zhang et al., J. Phys. Chem.: B **102** (1998) 10871-10878.
[9] Q. Li et al., J. Am. Chem. Soc. **133** (2011) 10878-10884.
[10] P.K. Dubey et al., Int. J. Hydrogen energ. **39** (2014) 16282-16292.
[11] L.Y. Ozer et al., J. Photochem. and Photobiol. C: Photochem. Rev. **33** (2017) 132-164.
[12] A.Zh. Zhumabekov et al., Theoretical and Experimental Chemistry **55** (2020) 398-406.
[13] A.Zh. Zhumabekov et al., Bulletin of the University of Karaganda-Physics **93** (2019) 54-60.
[14] H. Zhang et al., J. Li ACS Nano **4** (2010) 380-386. .
[15] G. Williams et al., ACS Nano **2** (2008) 1487-1491.
[16] M. He et al., Jour. Materials Chem. **22** (2012) 24254-24264.
[17] J.D. Roy-Mayhew et al., ACS Nano **4** (2010) 6203-6211.

[18] Q.B. Zheng et al., Carbon **49** (2011) 2905-2916.
[19] J. Zhang et al., Environmental Technology (2019) 1-13.
[20] S. Sreeja, K. Vidya Shetty, Environ. Sci. Pollut. Res. **23** (2016) 18154-18164.
[21] T. Wang et al., Physica E **112** (2019) 128-136.
[22] N.Kh. Ibrayev et al., Material Research Express **6** (2019) 1-11.
[23] D.A. Afanasyev et al., Russ. Jour. Phys. Chem. A. **90** (2016) 833-837.
[24] V. Swamy et al., Phys. Rev. B **71** (2005) 184302-12.
[25] W. Zhang et al., Angew. Intern. Edit. Chem. **48** (2009) 5864-5868.
[26] B. Zhang et al., J. Sci. Rep. **3** (2013) 1836-1843.